Order versus Temperature in Cholesteric Liquid Crystals from Reflectance Spectra

Dwight W. Berreman and Terry J. Scheffer*
Bell Telephone Laboratories, Murray Hill, New Jersey
(Received 20 October 1971)

The temperature dependence of specular-reflectance spectra of obliquely incident light reflected by a single-domain sample of a cholesteric liquid crystal in the wavelength range covering the first- and second-order Bragg reflection bands has been studied. The sample was a mixture of 4, 4′ bis(*n*-hexyloxy)azoxybenzene and optically active 4, 4′bis (2-methylbutoxy) azoxybenzene. The spectra of this sample are consistent with the Oseen-DeVries spiraling dielectric-tensor model and reveal that local dielectric tensors are ellipsoids of revolution to within our limits of resolution. Increasing the temperature increases the libration of the molecules and hence decreases the order parameter. This causes a decrease in eccentricity of the dielectric tensor which, in turn, produces readily measurable changes in the Bragg reflectance spectra. The observed changes are roughly in agreement with those predicted by assuming that the Maier-Saupe theory for temperature dependence of the order parameter in nematic liquid crystals also applies to cholesterics. We find it necessary to include a thermal-expansion coefficient to fit the data.

DESCRIPTION OF EXPERIMENT

The specular-reflectance spectrum of light reflected by a thin single domain of a mixed cholesteric liquid crystal has been measured at six different temperatures. The temperatures ranged from 69.4 to 93.5 °C. The transition to the isotropic phase occurs at 95 °C. At temperatures below about 65 °C part of the mixture crystallizes. The mixture contained 56.81% by weight of 4, 4′ bis (*n*-hexyloxy) azoxybenzene, which has a nematic phase, and the rest was optically active 4, 4′bis (2-methylbutoxy) azoxybenzene (MBAB) (see Fig. 1). The MBAB does not have a liquid-crystal phase by itself but it imparts a cholesteric twist to the nematic.[1,2]

This liquid-crystal mixture differs from some of the cholesterol-derived cholesteric liquid crystals of recent commercial interest in that there is almost no change of the pitch of the spiral periodic structure with temperature in our mixture. We are interested in the temperature variation of the magnitude and dispersion of the axes of the local optical dielectric tensor, rather than gross changes in the periodicity of the structure.

The apparatus used to measure the sample was similar to that described in our earlier papers[2] except that the sample was confined between a fused-quartz optical flat and the optically flat surface of a fused-quartz hemisphere (as shown in Fig. 2) rather than between two glass prisms. The new arrangement allowed us to vary the azimuthal angle and angle of incidence of the light with respect to the sample easily without changing the sample, although these parameters were held constant in the experiments reported here.

The optical flat and the hemisphere were both rubbed on lens tissue in the "*y*" direction, normal to the plane of the incident and reflected light beams (see Fig. 2). This caused the major axis ϵ_{22} of the optical dielectric tensor of the liquid crystal adjacent to the two surfaces to be aligned in the *y* direction (see Fig. 3). The ϵ_{22} axis coincides with the local preferred direction of the molecules shown in Fig. 1.

Figure 4 shows the image of blue light reflected at 45° from the sample. The image was photographed at the opaque mask. The aperture in the mask selects the area of the sample where reflectance is to be measured (see Fig. 2). The bright

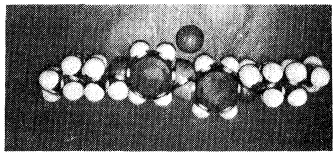

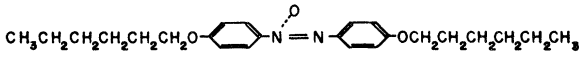

4,4'-BIS(n-HEXYLOXY) AZOXYBENZENE

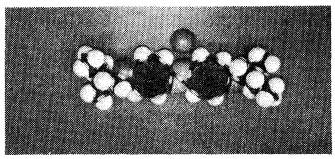

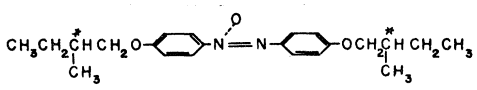

dextro 4,4'-BIS(2-METHYLBUTOXY) AZOXYBENZENE

FIG. 1. Two types of molecules in the cholesteric-liquid-crystal mixture.

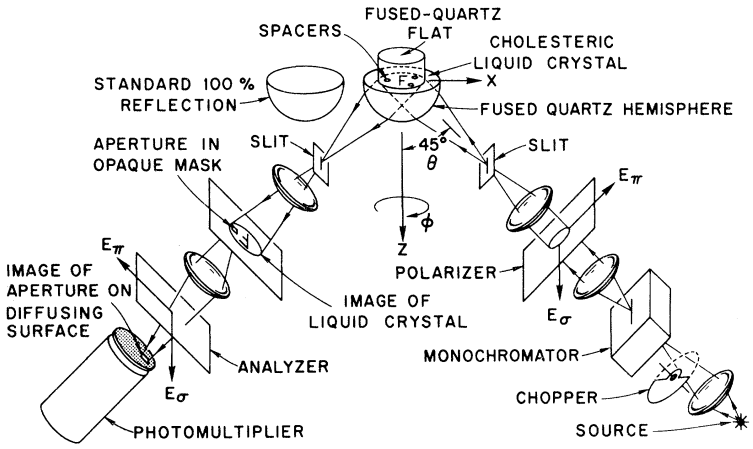

FIG. 2. Schematic diagram of apparatus for measuring reflectance spectrum of a single domain in a liquid-crystal film with oblique light.

spots on Fig. 4 are from light totally internally reflected in the hemisphere at the location of two bubbles adjacent to the sample area. The striped pattern comes from periodic, sawtooth variation in pitch of the sample. There are sudden steps, or Grandjean-Cano[3,4] discontinuities, where the number of turns of the dielectric tensor as it spirals from one surface to the other, as shown in Fig. 3, changes by one-half. The discontinuities are the approximately straight, slightly jagged lines between light and dark areas. The pitch variation occurs because the flat and the hemisphere are not absolutely parallel, and there is room to accommodate more turns of the helix at the thicker side than at the thinner one. The discontinuities projected on the mask make a contour map of the sample thickness. The color of the monochromatic light for Fig. 4 was chosen so that it was near the wavelength for second-order Bragg reflection by the periodically varying dielectric sample. The pitch is such as to yield strong Bragg reflection on one side of each stripe but on the other side the pitch is too long to give much Bragg reflection.

We were able to demonstrate the validity of the Oseen-DeVries[5,6] model for the dielectric tensor in this cholesteric liquid crystal. According to this model, one principal axis of the dielectric tensor is always parallel to the sample surfaces and it spirals with constant pitch about an axis normal to the surfaces. The axes of the tensor are of the same magnitude everywhere in the crystal (see Fig. 3). In addition, we have demonstrated that the other two principal axes of the dielectric ellipsoid are equal or differ by less than 2 or 3% in these samples. This verification came

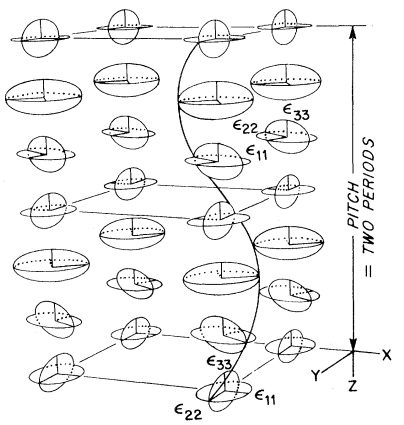

FIG. 3. Oseen-DeVries model of spiraling dielectric tensors in flat single domains of cholesteric liquid crystals.

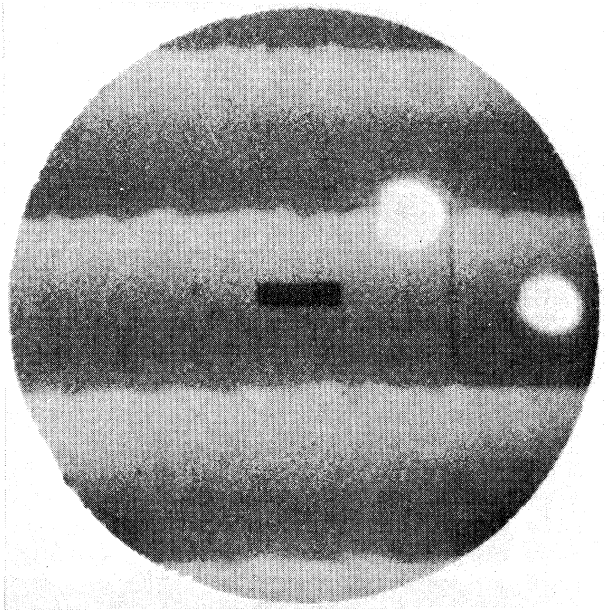

FIG. 4. Image of a cholesteric-liquid-crystal sample on the opaque mask. Two air bubbles, four Grandjean-Cano discontinuities, and the aperture centered between two discontinuities are visible.

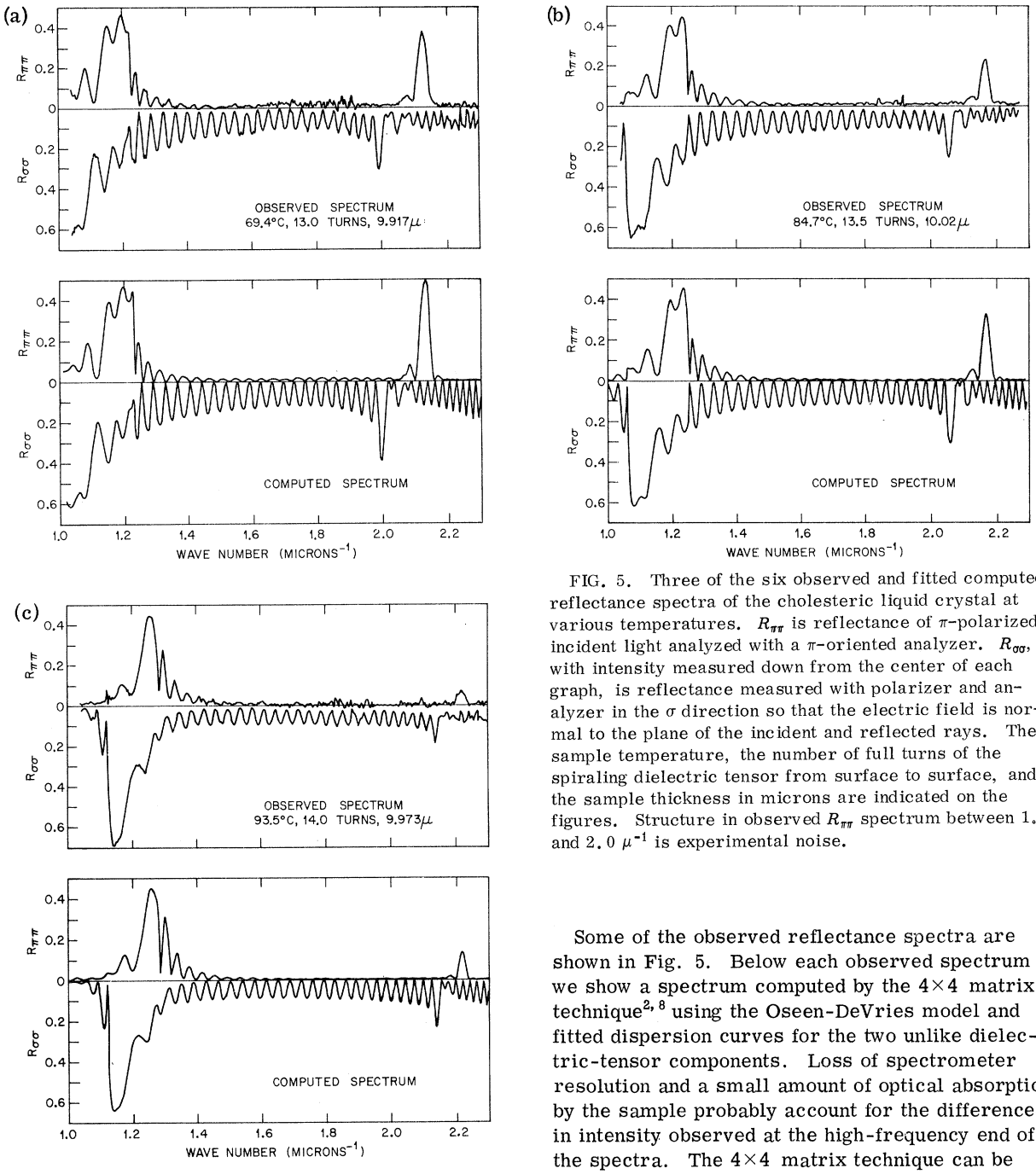

FIG. 5. Three of the six observed and fitted computed reflectance spectra of the cholesteric liquid crystal at various temperatures. $R_{\pi\pi}$ is reflectance of π-polarized incident light analyzed with a π-oriented analyzer. $R_{\sigma\sigma}$, with intensity measured down from the center of each graph, is reflectance measured with polarizer and analyzer in the σ direction so that the electric field is normal to the plane of the incident and reflected rays. The sample temperature, the number of full turns of the spiraling dielectric tensor from surface to surface, and the sample thickness in microns are indicated on the figures. Structure in observed $R_{\pi\pi}$ spectrum between 1.6 and 2.0 μ^{-1} is experimental noise.

about through our success in matching the observed spectra with spectra computed on the basis of the model. Only a poorer match was obtainable when we altered the model so that the pitch was nonuniform or so that the two minor axes of the dielectric tensor were nondegenerate. Poorer fits were also obtained when the tensor axes were assumed to vary appreciably in magnitude with distance from the surfaces.[7]

Some of the observed reflectance spectra are shown in Fig. 5. Below each observed spectrum we show a spectrum computed by the 4×4 matrix technique[2,8] using the Oseen-DeVries model and fitted dispersion curves for the two unlike dielectric-tensor components. Loss of spectrometer resolution and a small amount of optical absorption by the sample probably account for the differences in intensity observed at the high-frequency end of the spectra. The 4×4 matrix technique can be applied to absorbing media but it becomes considerably more expensive to make computations because of the necessity of using complex numbers. The frequencies of spectral features are not appreciably affected when absorption is small, as in these examples. There is also some frequency-dependent random noise in the observed spectra. For brevity, spectra are shown at only the two extreme temperatures and one in the middle. Spectra were measured at six temperatures.

The optical dielectric dispersion curves that

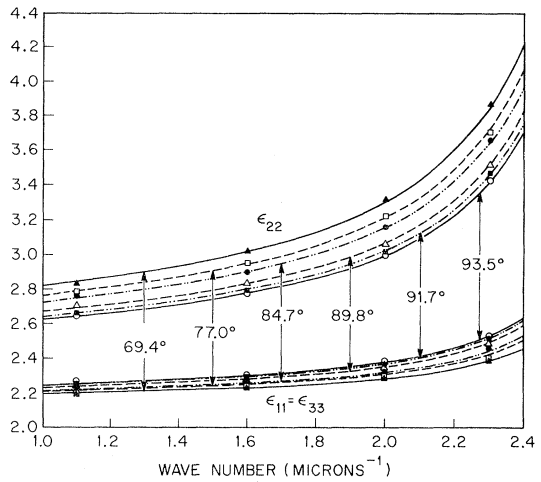

FIG. 6. Points are from optical dielectric dispersion curves computed from Eq. (7) to give the best fit to the observed reflectance spectra at six different temperatures. Curves are best fits consistent with Eqs. (3), (5), and (6).

gave the best fits to the data are shown in Fig. 6. In addition to the reflectance spectra it is necessary to know the sample thickness, the number of turns of the dielectric tensor from upper to lower surface, and the refractive index of quartz in order to get these curves. Sample thickness was obtained by a simple computation from measurements of the frequencies of 10–15 interference-fringe minima observed with monochromatized light of various wavelengths impinging normally through the optical flat on bubbles of air in the sample near the small region where reflectance was measured. Since the flat and the hemisphere were not absolutely parallel, the thickness was measured at two points, and thickness at the sampling point was obtained from interpolation. Measurements at three points was unnecessary because the Grandjean-Cano discontinuities showed the direction of steepest slope of the sample thickness.

The easiest way to determine the number of half-turns was to count the number of fringes between appropriate features in the two Bragg reflection bands in the observed spectra. One more fringe appeared for each additional half-turn. A wrong estimate of the number of half-turns gave obviously erroneous dispersion curves when attempts were made to fit the data. Another technique for getting the number of half-turns in the flat samples which gives an approximate result and is useful for an initial estimate, is to obtain the cholesteric pitch of another sample of the same material by measuring Grandjean-Cano discontinuities in a sample confined between a rubbed flat and a rubbed weak spherical lens. The number of half-turns is then the thickness of the flat sample divided by half that pitch.[2] The result is usually correct within half a turn.

The dielectric dispersion curve of fused quartz was obtained from a formula in the *International Critical Tables* (Ref. 9) and is shown in Fig. 7. Its temperature dependence is negligible.

INTERPRETATIONS

The purpose of this section is to present an oversimplified model to give an intuitive understanding of the thermal variation of the observed spectra. The model is able to describe the observed spectra extremely well with a minimum of parameters, but it should not be taken too literally.

Two more or less independent factors contribute to the temperature dependence of the dispersion curves (see Fig. 6). One is the thermal expansion of the liquid crystal. Although it produces a small effect, good fitting of the data with the semiempirical model to be described required its inclusion. The other factor is a sort of mean square degree of disoreintation of the individual long molecules in any one region from the "directrix." The directrix describes their average or preferred direction and coincides with the major axis of the dielectric tensor in that region. The amount of such disorientation can be approximately described by an order parameter S which is unity for perfectly parallel molecules and zero for perfectly disordered ones.[10] In defining such an order parameter we are implicitly ignoring bending of the molecules and the fact that there are two types of molecules. We are pretending that they are all identical ellipsoids of revolution whose dielectric properties and mechanical properties have coincident axes of symmetry Although this is quite a crude model it works re-

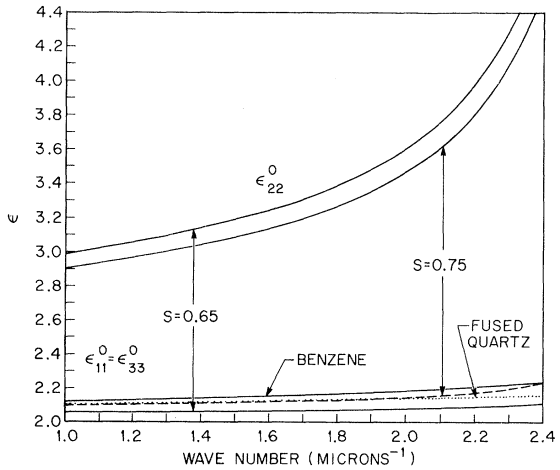

FIG. 7. Dispersion curves of ϵ^0_{ii} at 69.4 °C obtained from Eqs. (3), (5), and (6) and parameters in Table I. The outer curves are obtained assuming $S=0.65$, and the inner curves are obtained assuming $S=0.75$. Note that dispersion of the ϵ^0_{11} curve is closer to that of benzene when $S=0.75$ than when $S=0.65$.

markably well, at least for this material. The theory of Maier and Saupe[10–12] for nematic liquid crystals is based on the concept of such an order parameter.

We will suppose that the density of the liquid crystal can be described by the formula

$$\rho = \rho_c[1 + \alpha(T_c - T)] , \tag{1}$$

where ρ_c is the density just below the temperature of transition to the isotropic phase T_c, and α is the thermal-expansion coefficient.

We will also suppose that if the order parameter S is unity, then each principal axis of the optical dielectric tensor is related to the density through the Lorentz formula[13]:

$$(\epsilon_{ii}^0 - 1)/(\epsilon_{ii}^0 + 2) \propto \rho . \tag{2}$$

In doing this we are ignoring the anisotropy both of the dielectric tensor and of the thermal expansion. If we define one component of the same dielectric tensor just below the critical temperature as ϵ_i (still setting the order parameter at unity), then (1) and (2) can be combined to give

$$\epsilon_{ii}^0 \approx \epsilon_i + \tfrac{1}{3}[\alpha(T_c - T)(\epsilon_i^2 + \epsilon_i - 2)] . \tag{3}$$

The order parameter S is defined by the equation[10]

$$S = \tfrac{1}{2}\langle 3\cos^2\theta - 1\rangle , \tag{4}$$

where θ is the angle between the directrix and the long axis of the ellipsoid for any one molecule. It is not difficult to show from this definition, together with the assumption of negligible correlation for values of θ among neighboring molecules, that the dielectric tensor is smeared out to a more nearly isotropic shape according to the formulas

$$\epsilon_{11} = \epsilon_{33} = \tfrac{1}{3}[(2+S)\epsilon_{11}^0 + (1-S)\epsilon_{22}^0] , \tag{5}$$

$$\epsilon_{22} = \tfrac{1}{3}[(2-2S)\epsilon_{11}^0 + (1+2S)\epsilon_{22}^0] , \tag{6}$$

TABLE I. Two almost equivalent sets of parameters.

S (69.4 °C)	0.650	0.750
S (77.0 °C)	0.583	0.672
S (84.7 °C)	0.543	0.627
S (89.8 °C)	0.468	0.540
S (91.7 °C)	0.428	0.494
S (93.5 °C)	0.406	0.468
α	0.000 62	0.000 63
$A_{11}(\mu^{-1})$	0.0703	0.0919
A_{21}	2.0464	2.0655
A_{31}	0.0148	0.0372
$A_{41}(\mu^{-1})$	2.736	2.727
$A_{12}(\mu^{-1})$	0.2598	0.2563
A_{22}	2.3852	2.3647
A_{32}	0.5851	0.5285
$A_{42}(\mu^{-1})$	2.760	2.757

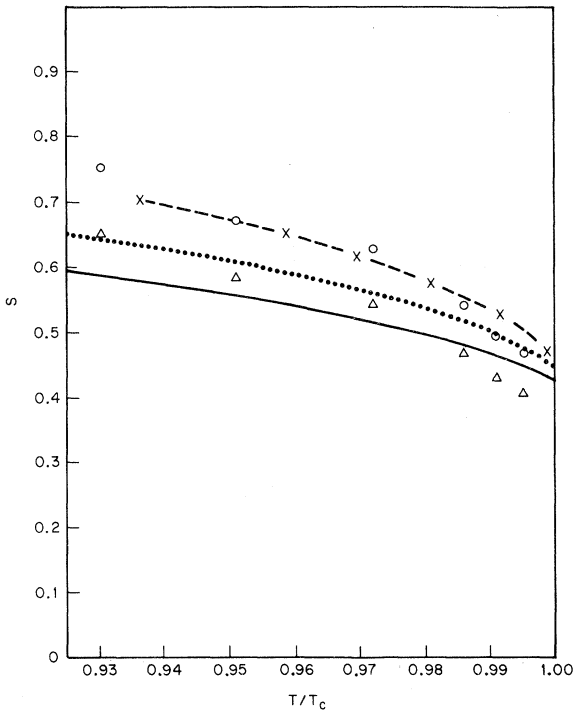

FIG. 8. Order parameter S as a function of relative temperature. The solid line is recomputed from the Maier-Saupe theory, neglecting thermal expansion. The dotted line is obtained from the theory using expansion properties of PAA. The two sets of unconnected points are obtained from our experiments assuming two different values of S at 69.4 °C: triangles for $S = 0.65$ and circles for $S = 0.75$. Dashed line is through points obtained from refractive indices of 4, 4′ bis (ethoxy) azoxybenzene (Ref. 11).

where we have chosen the subscript 2 to represent the unique axis of the tensor, as shown in Fig. 3.

Equations (3), (5), and (6) define the thermal dependence of the dielectric tensor in terms of a constant α and a temperature-dependent order parameter S. The success of the model is measured by seeing how good a fit can be obtained to all the data without attributing any other temperature dependence to ϵ_{ii}; that is, assuming that there is one temperature-independent dispersion function for $\epsilon_1 = \epsilon_3$ and another for ϵ_2.

We find that the model is quite good. We do not come up with one unique value of S at any one temperature, however, because we do not know what the dispersion curves ϵ_{ii}^0 are, and almost identical results can be obtained by fitting different curves of S vs T with different dispersion curves (see Table I and Figs. 7 and 8). However, if the theory is approximately valid, reasonable dispersion curves should be obtained for ϵ_i. It is unreasonable to expect $\epsilon_1 = \epsilon_3$ to be less dispersive than fused quartz for red and yellow light as it appears

to be if $S = 0.65$ at 69.4 °C (see Fig. 7). It is likely that its dispersion is more like that of pure benzene, since both molecules have two benzene rings. Using $S = 0.75$ at 69.4 °C gives a dispersion curve for ϵ_{11}^0 more similar to that of benzene.[9] Thus the upper set of points in Fig. 8 and the inner two dispersion curves in Fig. 7 are probably the best choice, assuming that the model is meaningful.

We found it convenient and sufficiently accurate to represent the dispersion of the dielectric-tensor components ϵ_i by the following classical harmonic oscillator dispersion function, which contains a far-infrared and a near-ultraviolet resonance term:

$$\epsilon_i = -(A_{1i}/\nu)^2 + A_{2i} + \{A_{3i}/[1 - (\nu/A_{4i})^2]\}. \quad (7)$$

The parameters S, α, and A_{ji} that yielded some of the curves in Figs. 7 and 8 are given in Table I. The second column in Table I is the one we regard as the best choice.

It is clear from Table I that the fitted value of the expansion coefficient α is practically independent of the choice of order parameter S. Although we have no independent measurement of α for our liquid-crystal mixture, the value obtained is about the same as that for many similar organic liquids.

As stated at the beginning, the pitch of the cholesteric spiral is relatively independent of temperature in this material. The pitch only varied from 0.763 μ per full turn at 69.4 °C to 0.712 μ at 93.5 °C (see Figs. 5). All measurements were made at regions approximately halfway between two Grandjean-Cano discontinuities, and hence the numbers probably represent unstrained values of the pitch.

In Fig. 8 we have also plotted the order parameter of 4, 4′ bis (*n*-ethoxy) azoxybenzene as a function of relative temperature. The data are from a graph in a paper by Saupe[12] and are derived from refractive-index measurements on the nematic phase of that material by Chatelain and Germain.[14] Although there are wide variations in the curves of S vs T/T_c for various compounds,[10,12] the moderately good agreement between that curve and the one we adopted as the best choice for our cholesteric liquid crystal of somewhat similar compounds may lend further credence to our choice.

There are few other measurements of order parameter based on optical data. The order parameter curve for the nematic compound plotted by Saupe from optical measurements agrees quite well with a curve for the same compound obtained from NMR data.[12] This agreement supports the approximate validity of the rigid-molecule model, at least for the nematic material, which is essential to the concept of a single order parameter.

In addition to the experimental curves of S vs T/T_c in Fig. 8 we have plotted two curves obtained from the Maier-Saupe theory[10–12] for nematic liquid crystals. The solid curve was obtained ignoring the effect of thermal expansion at the nematic to isotropic transition and in the nematic range. The dotted curve is from Maier and Saupe[10,12] using expansion properties of PAA (para-azoxyanisol),[11] showing the marked effect of small expansion terms on the theoretical results. Inclusion of expansion improves somewhat the agreement with experimental data. Expansion terms for most nematic and cholesteric liquid crystals are about alike.

ACKNOWLEDGMENTS

We wish to thank F. C. Unterwald, J. Morrison, and R. C. Hewitt for assistance in the experimental part of this work. We also thank Dr. W. L. McMillan and Dr. G. Meier for helpful discussions regarding the Maier-Saupe theory.

APPENDIX: DETAILED FITTING PROCEDURE

The final parameter-adjustment procedure used to fit the experimental reflectance curves was the following. We always specified the values of ϵ_{ii} at four wave-number values: $\nu = 1.1$, 1.6, 2.0, and 2.3 μ^{-1}, and interpolated between those values with the four-parameter dispersion function

$$\epsilon_{ii} = -(A_{1i}/\nu)^2 + A_{2i} + \{A_{3i}/[1 - (\nu/A_{4i})^2]\}. \quad (A1)$$

[The four A_{ji} parameters were written explicitly in terms of the four values of ϵ_{ii} and ν with complicated analytic expressions that we will omit. The apparent inconsistency of Eqs. (7) and (A1) with Eqs. (3), (5), and (6) turned out to be negligible.]

First, a set of such values of ϵ_{ii} were obtained by trial and error for each spectrum such that wave numbers of computed spectral features matched the observed ones to within about 0.001 μ^{-1}. These "raw" values of ϵ_{ii} are shown by the points on Fig. 6.

Then we adjusted the two values of ϵ_i at each of the four wave numbers, a value of the expansion coefficient α, and five of the six values of S using Eqs. (3), (5), and (6) with a nonlinear least-squares fitting program to get the best fit of "derived" values of ϵ_{ii} to the "raw" values. The dispersion curves from these "derived" values of ϵ_{ii} are the continuous curves in Fig. 6. Finally, reflectance spectra computed from these "derived" values of ϵ_{ii} were compared with the observed spectra to be sure the fits were still reasonably good. It is these "derived" curves, and not the "raw" fitted curves, that are shown in the lower parts of Figs. 5. Almost identical sets of "derived" values of ϵ_{ii} were obtained for quite a wide range of choices of *one* of the values of S. Consequently, it was unnecessary to show a different set of curves like those

in Fig. 6 for different assumed values of S at 69.4 °C.

We also tried introducing a single small imaginary damping term $-i\gamma\nu/A_{4i}$ in the denominator of the oscillator term in brackets in Eq. (A1). We found that when the dimensionless damping parameter γ was 0.004 ± 0.0005, the computed intensities were the same as those observed at all temperatures, within experimental uncertainty. The computations took much more time with complex dielectric terms, and the frequencies of observed spectral features were not appreciably affected by such small damping. Consequently, nearly all the fitting was done ignoring optical absorption. Absorption was ignored in obtaining the computed spectra in Figs. 5.

---

*Now at Institut für Angewandte Festkörperphysik der Fraunhofer-Gesellschaft, 7800 Freiburg, West Germany.

[1]E. Sackmann, S. Meiboom, and L. C. Snyder, J. Am. Chem. Soc. 89, 5981 (1967).

[2]D. W. Berreman and T. J. Scheffer, Phys. Rev. Letters 25, 577 (1970); Mol. Cryst. Liquid Cryst. 11, 395 (1970).

[3]F. Grandjean, Compt. Rend. 172, 71 (1921).

[4]R. Cano, Bull. Soc. Franc. Mineral. Crist. 91, 20 (1968).

[5]C. W. Oseen, Trans. Faraday Soc. 29, 833 (1933).

[6]Hl. DeVries, Acta Cryst. 4, 219 (1951).

[7]In two recent abstracts for talks we attributed observed spectral features to failure of the Oseen-DeVries model. Before the talks were presented, we found that unexpectedly large spectral dispersion of the unique dielectric tensor axis accounted for these observations. See Bull. Am. Phys. Soc. 16, 332 (1971); and in Proceedings of the Optical Society of America, Spring Meeting Program, 1971 (unpublished).

[8]The 4×4 matrix technique was first described in integral form for flat layers with invariant dielectric tensors by S. Teitler and B. Henvis, J. Opt. Soc. Am. 60, 830 (1970). In Ref. 2 we described a differential form that is efficient for computations with continuously varying tensors.

[9]*International Critical Tables*, edited by E. W. Washburn (McGraw-Hill, New York, 1930), Vols. 6 (quartz) and 7 (benzene).

[10]W. Maier and A. Saupe, Z. Naturforsch. 13a, 564 (1958).

[11]W. Maier and A. Saupe, Z. Naturforsch. 15a, 287 (1960).

[12]A. Saupe, Angew. Chem. Intern. Engl. 7, 97 (1968).

[13]See, for example, G. Joos, *Theoretical Physics*, 2nd ed. (Hafner, New York, 1950), p. 452.

[14]P. Chatelain and M. Germain, Compt. Rend. 259, 127 (1964).

PHYSICAL REVIEW A VOLUME 5, NUMBER 3 MARCH 1972

Effect of Pressure on the Electron Mobility in Solid Helium†

V. E. Dionne,* R. A. Young,‡ and C. T. Tomizuka
Department of Physics, University of Arizona, Tucson, Arizona 85721
(Received 28 September 1971)

The effect of pressure on the mobility of the cavity-localized electron in solid helium has been studied to a pressure of 6660 atm. No delocalized electron state has been detected at this pressure below the melting point of the solid. It is shown that the results are consistent with the presence of electron bubbles at the highest pressures investigated. The nature of possible charge-trapping mechanisms that might account for the results is discussed.

INTRODUCTION

The study of properties of excess electrons in liquid[1-3] and gaseous[4,5] helium has received much attention during the past decade. The localized nature of the excess electron has been demonstrated both experimentally and theoretically. Its configuration as a bubble has been well established. With several exceptions, relatively little has been investigated in solid helium in which the electron is also localized. Keshishev, Mezhov-Deglin, and Shal'nikov[6] made preliminary measurements which have established a lower limit for the mobility of electrons in ^{4}He crystals. Cohen and Jortner[7] have extended theoretical considerations initially made for the liquid and gas phases to the problem of excess electrons in solid helium.

Within a broad range of helium densities the excess electron is self-trapped in a cavity whose radius is several times the interatomic distance. The cavity is the minimum free-energy configuration in helium associated with a weakly attractive long-range electron–helium-atom polarization potential and a strong short-range electron-atom re-

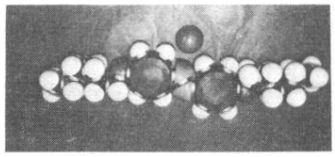

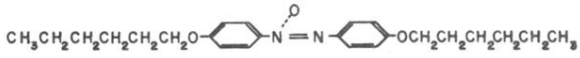

4,4'-BIS(n-HEXYLOXY) AZOXYBENZENE

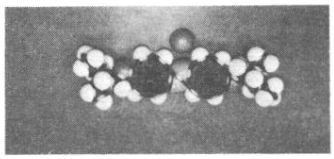

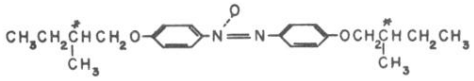

dextro 4,4'-BIS(2-METHYLBUTOXY) AZOXYBENZENE

FIG. 1. Two types of molecules in the cholesteric-liquid-crystal mixture.

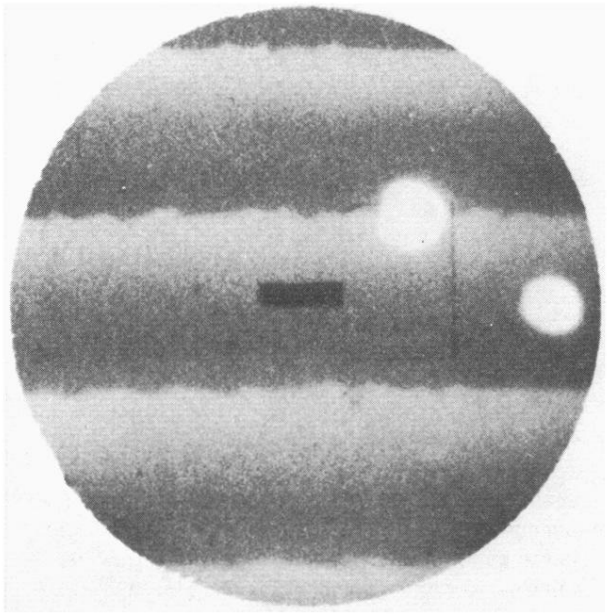

FIG. 4. Image of a cholesteric-liquid-crystal sample on the opaque mask. Two air bubbles, four Grandjean-Cano discontinuities, and the aperture centered between two discontinuities are visible.